PCCP



View Article Online **PAPER**



Cite this: Phys. Chem. Chem. Phys., 2021. 23. 10487

Toward a microscopic model of light absorbing dissolved organic compounds in aqueous environments: theoretical and experimental study†

Natalia V. Karimova, 📭 Michael R. Alves, 🕩 Man Luo, Vicki H. Grassian 🕩 *bc and R. Benny Gerber ** ** ** Add ** ** Add ** ** Add **

Water systems often contain complex macromolecular systems that absorb light. In marine environments, these light absorbing components are often at the air-water interface and can participate in the chemistry of the atmosphere in ways that are poorly understood. Understanding the photochemistry and photophysics of these systems represents a major challenge since their composition and structures are not unique. In this study, we present a successful microscopic model of this light absorbing macromolecular species termed "marine derived chromophoric dissolved organic matter" or "m-CDOM" in water. The approach taken involves molecular dynamics simulations in the ground state using on the fly Density Functional Tight-Binding (DFTB) electronic structure theory; Time Dependent DFTB (TD-DFTB) calculations of excited states, and experimental measurements of the optical absorption spectra in aqueous solution. The theoretical hydrated model shows key features seen in the experimental data for a collected m-CDOM sample. As will be discussed, insights from the model are: (i) the low-energy A-band (at 410 nm) is due to the carbon chains combined with the diol- and the oxygroups present in the structure; (ii) the weak B-band (at 320-360 nm) appears due to the contribution of the ionized speciated form of m-CDOM; and (iii) the higher-energy C-band (at 280 nm) is due to the two fused ring system. Thus, this is a two-speciated formed model. Although a relatively simple system. these calculations represent an important step in understanding light absorbing compounds found in nature and the search for other microscopic models of related materials remains of major interest.

Received 18th December 2020, Accepted 7th April 2021

DOI: 10.1039/d0cp06554d

rsc.li/pccp

I. Introduction

Aquatic dissolved organic matter, or DOM, is the largest reservoir of reduced carbon in the world (comparable in weight amount to atmospheric CO₂). 1-5 Production of marine DOM (m-DOM) occurs largely near the ocean surface, where the microbial loop and runoff from terrestrial sources result in a large diversity of compounds and properties.^{6,7} This m-DOM can be concentrated at the surface by up to nearly ten-fold and is defined as dissolved organic material that can pass through a 0.2 µm filter.8-12 The diverse and dynamic makeup of m-DOM, such as those of structurally unknown fatty acids, proteins, and macromolecular species, makes characterizing DOM across environments notoriously difficult.13 It was shown that the concentration, pH, ionic strength, and nature of the counterion influence the size and shape of the dissolved organic species. 14-16 Overall, all these experimentally obtained data about the molecular characteristics (mass and size) of DOM and its fractions are very extensive, but at the same time, the results are strongly influenced by differences in experimental conditions and different methods do not give the same results. Furthermore, experimental studies have provided a detailed view of the molecular characteristics of it: thousands of distinct molecular formulas making up the whole of the m-DOM. 17-22

The fraction of DOM that absorbs ultraviolet (UV) and visible light is referred to as CDOM. CDOM can be found in many other places besides the sea surface microlayers. 23-26 The importance of CDOM to aquatic ecosystems and its optical properties has been well established in the literature. 27-29 They are effective photosensitizers^{30,31} and exhibit strong absorption

^a Department of Chemistry, University of California, Irvine, CA 92697, USA. E-mail: bgerber@uci.edu

^b Department of Chemistry and Biochemistry, University of California, San Diego, CA 92093, USA. E-mail: vhgrassian@ucsd.edu

^c Department of Nanoengineering and Scripps Institution of Oceanography, University of California, San Diego, CA 92093, USA

^d Institute of Chemistry and Fritz Haber Research Center, Hebrew University of Jerusalem, Jerusalem 91904, Israel

[†] Electronic supplementary information (ESI) available. See DOI: 10.1039/ d0cp06554d

Paper

bands extending into the visible spectral region. 32-41 Additionally,

Cochran et. al. found that some of the analyzed particles absorb light as they become pyrolyzed or fluorescence. This suggests light absorbing components in sea spray aerosol.³⁰ Typically, the absorption spectrum of CDOM is characterized by a smooth decrease from the ultraviolet across the visible. 41 These features make them responsible for the optical activity of natural waters in many cases and play a role in the Earth's radiative energy balance. The photochemistry of CDOM has been the subject of several studies. 42-44 It has been suggested that optical and photochemical properties of CDOM arises through electronic interactions among various chromophores from partially oxidized oligomeric materials. 42 Further investigations of these interactions are very important for better understanding photochemical processes occurring in the seawater surface. 43 Additionally, it is very important to find a realistic, hydrated model system to study the structural and optical properties of CDOM. A combination of experimental and theoretical approaches to investigate these systems may provide insights into these light absorbing compounds and their environmental relevance.

Water systems contain light absorbing organic compounds that initiate photochemistry which impacts biogeochemical cycles and the composition of the atmosphere. However, little is known about these chromophores especially those present in seawater. Theoretical studies on the optical properties of CDOM system are insufficient. Just a few studies have been published in the literature. 45,46 For example, hydroquinonequinone donor-acceptor (D:A) complexes have been used as a small model system to study structure, energetics, and visible-UV spectra of HA.45 That these model systems provide a spectrum like that of natural humic acids is consistent with the model of Del Vecchio and Blough.⁴⁷ The most important variable in determining the energy and intensity of absorption seems to be the ring-ring distance in these complexes. Another interesting theoretical work related to the origin of DOM optical properties was performed by Rosario-Ortiz and co-workers. 46 In this work, three-dimensional configurations of dissolved organic matter (DOM) were used to study if DOM forms thermodynamically stable molecular aggregates that as a result were potentially shielded from water solvent molecules. Computational results showed that molecular aggregates are weak and dissociate when placed in organic solvents (tetrahydrofuran, methyl tert-butyl ether). Time-dependent density functional theory calculations demonstrated long-wavelength absorbance for both model DOM chromophores and their molecular aggregates.⁴⁶

The lack of theoretical study of these complex systems can be explained by a number of challenges: (i) the poorly understood and complex chemical composition of m-DOM; (ii) system size (very large molecules that are more than 120 atoms⁴⁸⁻⁵³) - this fact makes the calculations very difficult, especially when solvent molecules need to be included and; (iii) solvent effects and possible water-CDOM interactions such as deprotonation process can affect the simulated spectrum significantly.54 Theoretical-experimental microscopic analysis of the photoabsorption spectra of large system was recently demonstrated in studies by Finlayson-Pitts and co-workers55,56 of

photochemistry of neonicotinoid films. However, for these systems, the composition and molecular structures were well known.

In this work, we combine theoretical simulations by molecular dynamics using tight-binding density functional theory and excited state methods, with experiments that unravel important features of the optical spectrum of organic matter from seawater. The experimental measurements of UV-Vis spectra were performed for m-CDOM with concentration of 100 mg L^{-1} in the solution of water at pH 4.7. The empirical data provide us information about the excited states, but the interpretation of these results is a complicated process, due to the complexity of the system. Therefore, theoretical simulation can be used to assist in the understanding of empirically measured spectral features and can provide useful information about: (i) nature of excited states; (ii) solvent effects; (iii) chromophores position, and (iv) contribution of speciated forms to the m-CDOM optical spectrum. Here, we provide a specific structural model for light absorbing DOM material in pure water. The optical absorption spectrum was calculated for a m-CDOM model in the gas phase and with including 100 water molecules. Additionally, the ionized model of m-CDOM was simulated. The structural and solvent effects were investigated in the ground state. Obtained theoretical results were compared with experimental data for m-CDOM.

The approach taken employs Ab Initio Molecular Dynamics (AIMD) simulations of the ground state using the DFTB density functional method for the potential energy surface,57 and the TD-DFTB method for the excited state.⁵⁸ These densityfunctional theory methods seem capable of describing systems such as treated here with sufficient accuracy, while being computationally efficient. Additionally, to understand the role of the different groups on the optical properties of the m-CDOM, theoretical fragmentation analyses were completed.

Here we present a molecular model and explore its detailed structure, absorption spectrum, the effects of solvation on the substance, and the microscopic mechanisms that govern the spectroscopic properties for a specific macromolecular species relevant to m-CDOM. This approach taken opens the way for similar treatment of other types of molecular species present within the more complex m-CDOM, since the capability to compute large model systems has been demonstrated. This should be able to map out a very broad range of macromolecular species within m-CDOM and other CDOM samples, an important effort in future studies.

II. Theoretical model for m-CDOM

The composition analysis performed for the m-CDOM sample showed the presence of hydrogen, carbon, oxygen and nitrogen atoms in the structure.³⁰ Therefore, the theoretical model should include similar components in the structure. The promising structure was suggested in 1997 by Seaton and coworkers.51 They study the mechanism of the incorporation of nitrogen into m-DOM from photolyzed trilinolein. The structure introduced on Fig. 1a was suggested as representative model for

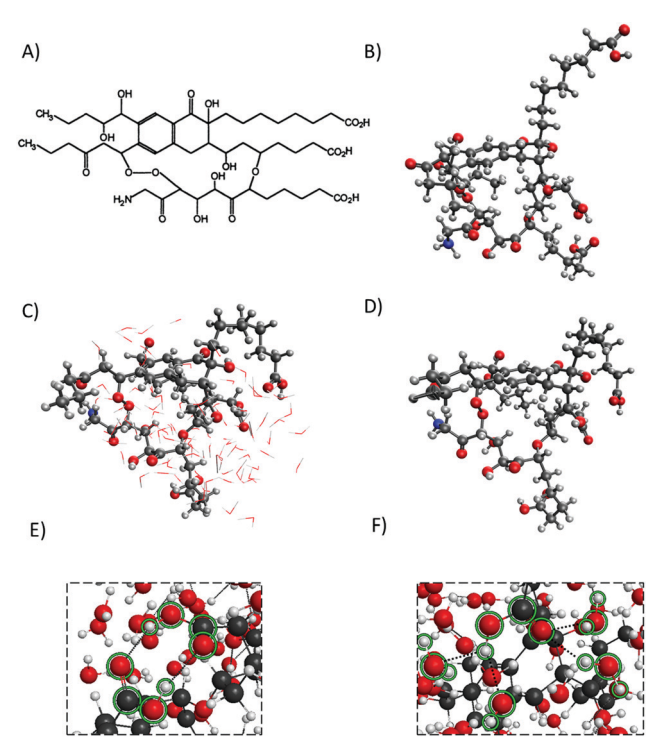


Fig. 1 Model system: (A) 2D structure of a model type compound within m-CDOM ($C_{48}O_{19}N_1H_{73}$); (B) simulated structure of the model of m-CDOM ($C_{48}O_{19}N_1H_{73}$) in gas phase. Structures (C) and (D) are related to the model of m-CDOM with including 100 water molecules $(C_{48}O_{19}N_1H_{73}\cdot(H_2O)_{100})$: water molecules are shown in (C) and hidden in (D). (E) Fragment of $C_{48}O_{19}N_1H_{73}$ · $(H_2O)_{100}$ with two groups -COOH interactions. (F) Water coordination around of -COOH group.

family of related structures containing covalent bound nitrogen that might be formed after photolysis (Fig. 1a).⁵¹

The preliminary calculations for this structure showed that optical spectrum of this neutral model is in good agreement with experiment even for isolate structure in a gas phase position of obtained bands are very close to experimental values (Fig. S1, ESI†). Therefore, in this work, the Seaton's structure is used as a model system to study optical effects, allowing us to figure out which chromophoric species is contributed to the formation of A-, B- and C-bands. Additionally, the influence of speciated forms and solvent effects on the optical absorption spectrum are considered. Therefore, three model systems were considered: (i) molecule C₄₈O₁₉N₁H₇₃ in a vacuum (Fig. 1a and b), (ii) solvated molecule C₄₈O₁₉N₁H₇₃·(H₂O)₁₀₀ (Fig. 1c and d), and (iii) ionized forms $(C_{48}O_{19}N_1H_{72}^-)\cdot (H_2O)_{100}$ (Fig. S2, ESI†).

A more detailed description about theoretical approaches and the structure calculations performed in this work can be found in Materials and methods.

III. Results and discussion

Experimental data

The UV-Vis spectrum for the aqueous extracted m-CDOM is similar to that for the terrestrial CDOM⁵⁹ with a continuous absorption increase starting from around 500 nm to below

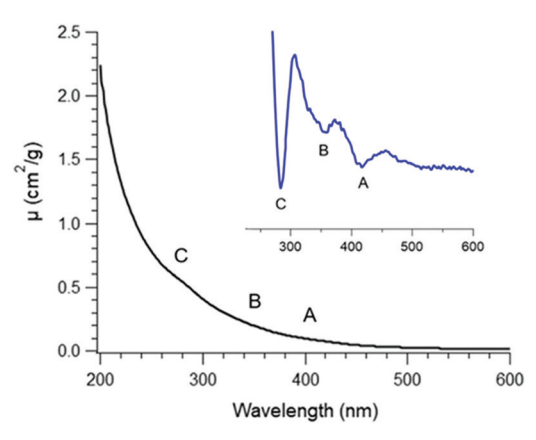


Fig. 2 Experimental mass absorption coefficient spectrum of m-CDOM in aqueous solution calculated from the UV-Vis spectrum. Inset: The inset shows the 2nd derivative of the spectrum to better identify peaks A, B and C that contribute to the broad spectrum.

200 nm. The mass absorption coefficient (μ) spectrum calculated from the UV-Vis spectrum can be seen from Fig. 2. There is one relatively obvious shoulder on the spectrum at around 280 nm (peak C). However, the second derivative curve (Fig. 2 insert) form the UV-Vis spectrum indicates there are three bands (A-C) and the wavelength range for these bands are summarized in Table 1.

Comparison theoretical and experimental results

In the first step, only the neutral forms C48O19N1H73 and $C_{48}O_{19}N_1H_{73}\cdot(H_2O)_{100}$ were used for simulations of the experimental spectrum of m-CDOM in water media. To consider the contribution to the total optical absorption spectrum of all possible structures, MD-DFTB trajectories were simulated for these two models. In the next step, obtained structures of along MD trajectories were used to calculate the total TD-DFTB optical absorption spectrum of model systems C48O19N1H73 and $C_{48}O_{19}N_1H_{73}\cdot(H_2O)_{100}$. Experimental electronic absorption spectrum recorded for water solutions of m-CDOM were compared with theoretical spectra of $C_{48}O_{19}N_1H_{73}$ and $C_{48}O_{19}N_1H_{73}$ · $(H_2O)_{100}$ model systems and are presented in Fig. 3.

The theoretical results obtained for the hydrated neutral model C₄₈O₁₉N₁H₇₃·(H₂O)₁₀₀ reproduce the experimental electronic A- and C-bands very well (Table 1 and Fig. 3): theory gives the correct range (390-420 nm) in accord with experiment for A-band and in the case of C-band, the difference in the position between theory and experiment is just 2 nm (theoretical C-band is located at 278 nm).

Table 1 Experimental optical absorption spectral data for m-CDOM and absorption characteristics within the broad band

Band	A	В	С
Wavelength (nm)	$410\pm20\;\text{nm}$	$350\pm20\;\text{nm}$	280 ± 3 nm

The weak experimental B-band between 320-360 nm (determined by second derivative analysis) was not theoretically reproduced by neutral model of m-CDOM. There are no strong

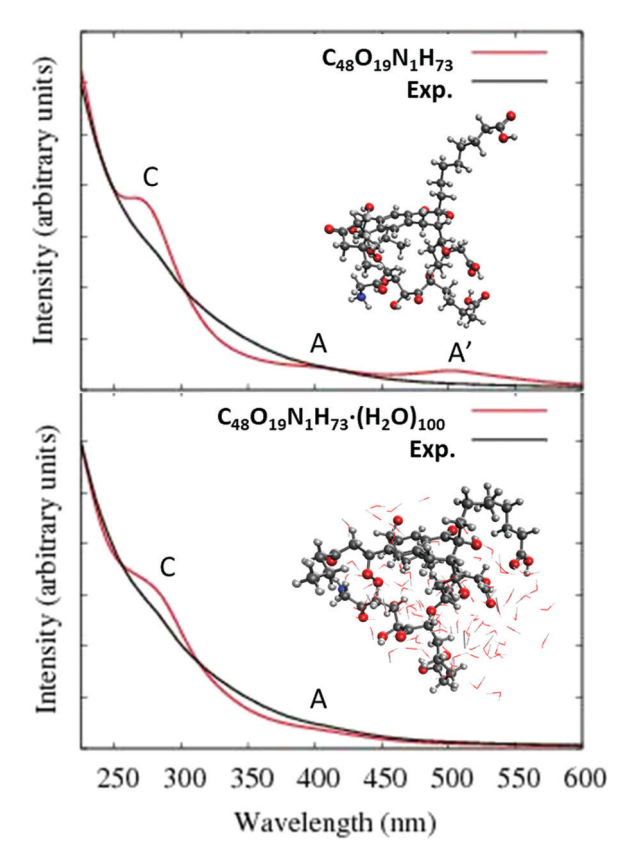


Fig. 3 The comparison experimental spectrum of a complex m-CDOM sample with total theoretical optical absorption spectra of gas-phase model m-CDOM component and its hydrated model.

excitations in the 320-360 nm region of simulated spectrum of $C_{48}O_{19}N_1H_{73}\cdot(H_2O)_{100}$ system (Fig. S3a, ESI†). However, the simulation of the optical spectrum of ionized forms of m-CDOM allowed us to localize the weak band in the region 300-370 nm (Fig. S2 and S3b-d, ESI†). Therefore, theoretical results showed that including the ionization process of the acid is important to reproduce the experimental spectrum. Obtained theoretical results for neutral and ionized m-CDOM models correctly reproduce the Franck-Condon region and excited states (A-, B- and C-bands). Considered theoretical and experimental approaches can be applied to other systems to gain a deeper understanding of optical and photochemical properties.

Solvent effects

Molecular dynamics results demonstrated that the presence of water molecules in the model affects the structure of the C₄₈O₁₉N₁H₇₃ molecule: it becomes more compact than an isolated molecule in the gas phase. Selected structures of $C_{48}O_{19}N_1H_{73}$ and $C_{48}O_{19}N_1H_{73}\cdot (H_2O)_{100}$ are presented in Fig. 1b-d. Ionization of the considered molecule was not detected during 15 ps in all MD trajectories.

Additionally, it was detected that solvent effects play an important role to the quality of the optical spectrum of C₄₈O₁₉N₁H₇₃ molecule. Both simulated spectra (C₄₈O₁₉N₁H₇₃ in the gas phase and the $C_{48}O_{19}N_1H_{73}\cdot(H_2O)_{100}$ hydrated model)

exhibits A- and C-bands (Fig. 3) as well as the experimental curve. However, an extra low-energy A'-band around 510 nm was detected for isolated C48O19N1H73 molecule in the gas phase. To understand the nature of this band the analysis of the structures contributed to the total theoretical optical spectrum was performed. It was detected that 84% of all structures do not have the A'-band at 510 nm, and 16% structures exhibit it. The main difference between these two types of structures may be related to the distance between two oxygens in peroxy-group $R_{\rm (O-O)}$: for structures with A'-band the $R_{\rm (O-O)} \approx 2.0$ Å, whereas in other cases it is much shorter and close to 1.5 Å.

To test this hypothesis, we selected one structure of $C_{48}O_{19}N_1H_{73}$ molecule in the gas phase with short $R_{(O-O)}$ = 1.5 Å (Fig. S4a, ESI†). Then the $R_{(O-O)}$ distance was increased till 2.0 Å and frozen (the rest of the molecule atoms were relaxed), Fig. S4a (ESI†). The optical absorption spectra of these two structures $(R_{(O-O)} = 1.5 \text{ and } 2.0 \text{ Å})$ can be found in Fig. S4b (ESI†). Results confirmed that A'-band appears when distance $R_{\rm (O-O)}$ increased to 2.0 Å. Also, it was detected that the nature of LUMO orbital is different in these structures (Fig. S4c and d, ESI†). The LUMO of structure with $R_{(O-O)} = 1.5 \text{ Å is } \pi^*$ -orbital, localized on the rings of the central part of the molecule (Fig. S4c, ESI†). Whereas the structure with $R_{(O-O)} = 2.0 \text{ Å has}$ the LUMO orbital which is delocalized on the right part of the molecule (Fig. S4d, ESI†), and non-bonding character of this orbital can be observed in the peroxide-fragment.

It should be noted, that for the hydrated model the number of structures with distance $R_{\rm (O-O)}$ closed to 2.0 Å (and lowenergy band between 450 and 600 nm) is less than 1% and they do not have a significant impact into the total optical spectrum. Therefore, solvent effects are very important for reproducing the correct observed optical spectra of m-CDOM.

Analysis of bands of m-CDOM spectrum

To understand the origins of the A-, B- and C-bands on the optical spectrum of m-CDOM, theoretical analysis of the excited states in the spectral region 250-450 nm of suggested models were performed. The theoretical absorption spectra for these structures consist a number of weak and closely spaced excited states, particularly at higher energies. Therefore, to simplify the spectral analysis of the absorption spectrum, only the excited states with oscillator strengths higher than $f \approx 0.003$ will be considered.

Results showed, that orbitals involved into the formation of the A- and C-bands of neutral C₄₈O₁₉N₁H₇₃ and C₄₈O₁₉N₁H₇₃. (H₂O)₁₀₀ model systems are very complex (see ESI,† Fig. S5 and S6), especially for the hydrated system when orbitals of water molecules are also participating. Despite this, there are some similarities in orbital character for the $C_{48}O_{19}N_1H_{73}$ and $C_{48}O_{19}N_1H_{73}\cdot (H_2O)_{100}$: there are $\pi\to\pi^*$ transitions for the most part of the spectrum (Fig. 4 and Fig. S5, S6, ESI†). The B-band (obtained for ionized structures) arises from the combination of $n \to \pi^*$ and $\pi \to \pi^*$ transitions.

Chromophores within m-CDOM

Unfortunately, it is difficult to clearly identify the roles of different atoms in the formation of bands, using only orbital

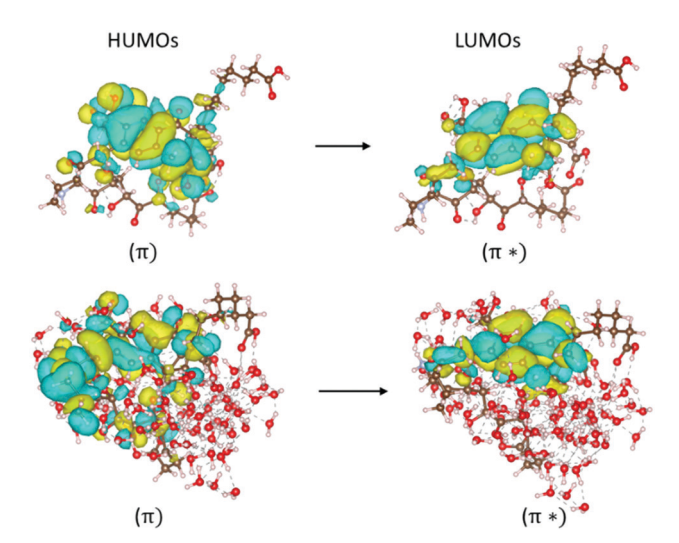


Fig. 4 Example of the $\pi \to \pi^*$ electron transitions in the model systems: $C_{48}O_{19}N_1H_{73}$ and $C_{48}O_{19}N_1H_{73}\cdot(H_2O)_{100}$

analysis. To understand the contribution of different fragments of the molecule on the formation of spectral bands, theoretical fragmentation analysis was performed. Due to the fact that the B-band is very weak in the spectrum and contribution of the ionized form into the total optical HS spectrum is not significant, this analysis was performed only to study the nature of the strongest A- and C-bands. One isolated structure of C48O19N1H73 in a gas phase was selected from MD trajectories. We choose the conformer with distance $R_{(O-O)} = 1.5 \text{ Å}$, to eliminate the formation of low-energy A'-band (at 510 nm), which arises due to the steric effects between long carbon chains in a gas phase. The spectrum of this model is shown in Fig. 5a.

Then, all carbon chains were substituted by the hydrogen atom (without further geometry optimization). The optical absorption spectrum of obtained structure can be found in Fig. 5b. These groups influence the A-band position, which became blue-shifted for the structure without carbon chains. The absence of amino group (-NH2) does not affect the spectrum of this model (Fig. 5c). After diol- and oxy-groups were deleted, A-band disappears (Fig. 5d). Therefore, we can conclude that A-band is mainly formed by diol- and oxy-groups (the first detected chromophore in this molecule) together with carbon chains. Additionally, we detected that the central two rings are a second chromophore and responsible for the formation of C-band at 275 nm (Fig. 5e).

We want to notice that there are different points of view on the possible structure(s) of chromophoric dissolved organic matter: (1) the CDOM can be considered as composed of macromolecules,⁵¹ and (2) CDOM is composed of aggregates of smaller species⁴⁶ bonded by non-covalent interactions. In the current study, we investigated a single macromolecular species as a model for a large light absorbing molecule within the complex m-CDOM sample. Interestingly, the model showed that the fragmentation analysis, i.e. the combination of the smaller fragments of this molecule, could be considered one of several possible successful model toward starting to

understand these complex systems from a fundamental perspective. In future work, we are planning to perform the calculations on aggregates of fragments as well.

Additionally, one of our future goals is developing theoretical model which includes coordinating ions present in seawater. The ions are expected to interact with m-CDOM, 60 which can impact the optical and photochemical properties. Taking the seawater ions into account can make the marine system models more representative and further the goal towards finding insights through microscopic investigations of marine-relevant chromophoric dissolved organic matter in aqueous salt solutions.

IV. Conclusions

In the present work, experimental spectroscopic measurements are combined with theoretical calculations to study the optical absorption spectra of m-CDOM in aqueous solution. The hydrated model provides a good agreement with the experiment, in particular: correct Franck-Condon region and correct excited states. Solvent effects are important for reproducing the correct optical spectra of m-CDOM in the water environment.

The analysis of the contribution of different molecule fragments to the formation of spectral bands allowed us to identify the chromophores position in the considered model system. Two chromophores were found: (i) the low-energy A-band arises due to the diol- and the oxy-group combined with carbon chains; (ii) the higher-energy C-band appears due to the two condensed rings. Also, theoretical results showed that there are $\pi \to \pi^*$ transitions for the most part of the spectrum for both gas phase and hydrated molecules. We demonstrated that the contribution of all speciated forms to the total absorption spectrum is essential: the deprotonated species of m-CDOM contributes to the formation of the weak B-band, which arises from the combination of the $n \to \pi^*$ and $\pi \to \pi^*$ transitions. Overall, we can conclude that the combination of the excited states quantum chemistry with molecular dynamics provides a very good interpretation of the experiment, and the results demonstrate the possibility of a microscopic understanding of the absorption spectra of complex organic molecules in water by calculations.

Due to the complexity and wide varieties of possible molecular structures, it is very likely that there are many different molecular structures and fragments contributing to the absorption spectrum. These results are important because calculations for realistic models are now feasible. The future will be to compare with more experiments and consider additional models informed by detailed analyses of the molecular components of m-CDOM. Ultimately, we will identify the most promising model, which can provide some initial understanding of these complex light-absorbing substances' optical properties. The theoretical approach developed in this paper can be applied to test other models of complex macromolecular structures found in environmentally complex systems.

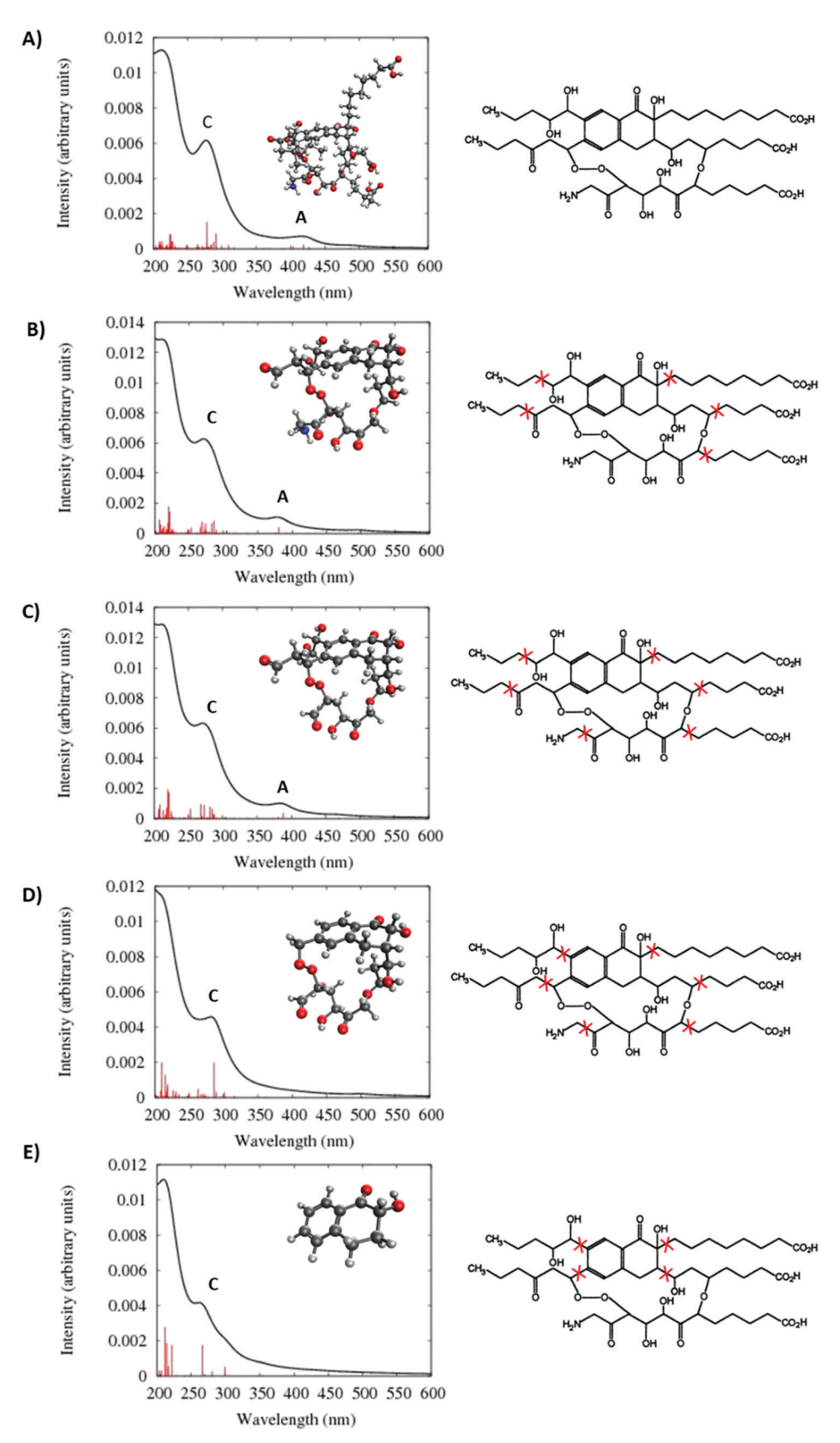


Fig. 5 Calculated optical absorption spectra of different fragments of the m-CDOM molecule in gas phase: (A) the entire molecule; (B) carbons chains were removed; (C) amino-group was additionally deleted; (D) diol- and oxy-groups near the ring were additionally removed; and (E) only two condensed rings were considered.

V. Materials and methods

Methods for m-CDOM collection

The m-CDOM used in this study was collected from a large scale mesocosm experiment, known as SeaSCAPE (Sea Spray Chemistry and Particle Evolution) 2019, in which a monitored microbial bloom was allowed to progress through its growth and death stages. Briefly, the experiment was performed in a large 15 000+ liter wave flume tank61 and additional details regarding this study will be discussed in a forthcoming publication. Nutrients were added to facilitate this bloom including f/2 algae growth medium (Proline, Aquatic Eco-Systems) and sodium metasilicate solutions. Water from the end of the bloom cycle was collected and gravity filtered through a series of 50, 10, 1, and 0.2 micron pore-size filters. The extraction and purification process for obtaining m-DOM is described by Dittmar and co-workers.⁶² Briefly, the filtered seawater is acidified to, or close to, a pH value of 2.0 using 1 M HCl (Sigma Aldrich). This solution is then pass through a solid phase extraction column (Bond Elut PPL, Agilent) at a rate of no more than 5 mL min⁻¹ or 2 drops per second. Once the extraction is finished, the column is subsequently washed with Milli-Q water multiple times and the m-CDOM is eluted with methanol. The dark yellow/orange m-CDOM solution is quickly dried down and stored at −21 °C under nitrogen to prevent any methylation or changes in the m-CDOM chemistry. All glassware used during this process was combusted at 500 °C to remove any trace organics.

Methods for UV-Vis experiments

UV-Vis spectral information of m-CDOM was obtained using a Shimadzu UV-3600 UV-VIS-NIR spectrophotometer in the wavelength range from 200 to 600 nm. The m-CDOM solution was prepared as 100 mg L⁻¹ using Milli-Q water with and electric resistance of 18.2 M Ω . The pH of the solution was not adjusted, and the pH of the unadjusted solution was determined using an Oakton 700 pH meter.

Theoretical methods

Due to the system size especially when solvent molecules are included, the calculation of excited states using traditional ab initio approaches are very challenging. One possible method that can accurately describe structural and optical effects in large systems with the reasonable computational cost is the density functional tight-binding (DFTB) method⁵⁷ and excited states formalism TD-DFTB, 57,58 which aims to achieve the accuracy of DFT methods and the efficiency of tight-bindingbased methods. The performance of approximate quantum mechanical methods such as AM1, PM3 and DFTB in their description of conjugated Schiff base models were tested by Elstner and co-worker. 63 The results obtained from DFTB calculations are very close to those obtained from full DFT: the structures, bond alternations and isomerization barriers can be properly described within DFTB. Its overall performance is better than semiempirical methods like MNDO, AM1, and PM3. The TD-DFTB method has been successfully applied to predict the optical properties and excited-state electron

dynamics of large systems, such as Ag:DNA clusters,64 semiconductor nanoparticles,65 silver nanoparticles66 and others.

In current work, all calculations were performed using the DFTB+ (18.2 version) package.⁶⁷ The calculations were performed using the DFTB3-D3H5 formalism^{68,69} and the 3ob-3-1 parameter set. 70-73 DFTB-D3H5 is a variant of DFTB3 with additional corrections for non-covalent interactions (dispersion and hydrogen bonds). For a DFTB3-D3H5 calculation, a specific parametrization of the dispersion correction (DftD3) has to be used: $sr_6 = 1.25$; alpha₆ = 29.61; $s_6 = 1.0$; and $s_8 = 0.49$.⁶⁹ In addition, the hydrogen-hydrogen repulsion was also activated.⁷⁴ The maximum angular momenta was set to: H = s; C = p; O = p; and N = p. The Hubbard derivatives (in atomic units) were specified for selected parameter set: H = -0.1857; C = -0.1492; O = -0.1575; and N =-0.1535.

Excited states of the molecule (C₄₈O₁₉N₁H₇₃) in a gas phase and with including water molecules (C48O19N1H73:(H2O)100) were calculated using TD-DFTB method⁵⁸ as implemented in the DFTB+ package. To include all possible speciated forms into the total optical spectrum the combinations of MD-DFTB with TD-DFTB were suggested (see a more detailed description of this approach below in the next section). All MD calculations were performed at constant energy. Initial velocities were sampled for the equilibrium structure of interest from a Boltzmann distribution at 298 K. A time-step was 0.4 fs. We simulated 100 trajectories for C₄₈O₁₉N₁H₇₃ in gas phase and 100 trajectories for hydrated system C₄₈O₁₉N₁H₇₃·(H₂O)₁₀₀ (total time around 15 ps per trajectory). Each of these trajectories was used for calculation total optical absorption spectrum: we extracted structures every 250 fs of the simulation, and their vertical excitation energies and oscillator strengths were calculated with TD-DFTB. For each excitation energy, the vertical transitions were convoluted with a Lorentzian line shape with a width of 35 nm, and all the resulting Lorentzians were added to yield the excitation spectrum. This approach was previously used by Gerber group for simulation of β-hydroxyalkyl nitrates, pyruvic and benzoic acids. 54,75-77

For hydrated m-CDOM model (C₄₈O₁₉N₁H₇₃·(H₂O)₁₀₀), the pairs of occupied and virtual orbitals with oscillator strengths of the single-orbital transitions less than 10⁻³ were eliminated from the guess vector of the excited states. The threshold is often necessary for large systems, since the number of excited states that must be calculated to obtain a spectrum can be extremely high.66 The threshold does not significantly affect the quality of the theoretical spectrum, however, allowed significantly reduces computational costs (see Fig. S1, ESI†).

Additionally, contribution of ionized form of m-CDOM model into optical absorption spectrum was studied. Several ionized light absorbing molecules (C₄₈O₁₉N₁H₇₂⁻)·(H₂O)₁₀₀ were simulated. Geometry optimization procedure performed with DFTB. Then obtained geometries were used to calculated vertical excitation energies to simulate the spectral region between 300-370 nm using TD-DFTB.

Theoretical models for m-CDOM

• Gas phase structures of neutral C₄₈O₁₉N₁H₇₃. To get structures used for calculation of the optical absorption spectrum, the initial guess structure of $C_{48}O_{19}N_1H_{73}$ molecule was optimized using DFTB method. This obtained geometry was used to run a long trajectory of 250 ps (a time-step of 0.4 fs) at constant energy. Then, 10 the most energetically preferable conformers from the trajectory were selected. The geometry of each of these conformers was relaxed by DFTB and then used as an initial structure to run 10 short trajectories at constant energy, total time is around 15 ps and a time-step is 0.4 fs. Therefore, 100 trajectories were simulated for $C_{48}O_{19}N_1H_{73}$ system in a gas phase. Structures obtained from these 100 trajectories were used to perform TD-DFTB calculations.

• Hydrated model of C₄₈O₁₉N₁H₇₃. To choose the proper solvent model for the current system, two possible ways to incorporate solvent effects were considered: (a) combination of a small amount of explicit water molecules with the polarizable continuum model, and (b) a large amount of explicit water molecules only. The molecule of 4-benzoylbenzoic acid (4BBA) was chosen to provide a chromophore model to test these two models (Fig. S7a and b, ESI†). 4BBA is smaller than m-CDOM we study here but large enough to provide a suitable test case for these two approaches. Obtained results found that for organic acids with different functional groups in the structure, even the combination of a small number of explicit water molecules and implicit solvation was not sufficient and did not allow us to reach an agreement with the experiment. These systems require a significant amount of explicit water molecules to mimic the experimental optical spectrum (Fig. S8a and b, ESI†). A more detailed description about these theoretical results can be found in the ESI,† Solvent model justification pp. S8-S9.

Therefore, to generate possible hydrated structures of m-CDOM we considered a model of C48O19N1H73 coordinated by 100 explicit water molecules. Packmol⁷⁸ program was used by randomly inserting 100 water molecules and the C₄₈O₁₉N₁H₇₃ (ten the most energetically preferable structures obtained in gas phase calculations) into a sphere of radius 9 Å. Geometries of these ten C₄₈O₁₉N₁H₇₃·(H₂O)₁₀₀ structures were optimized by DFTB and used to run 10 short trajectories at constant energy per structure (total 100 trajectories), with total time up to 15 ps and a time-step is 0.4 fs. Structures obtained from these 100 trajectories were used to perform TD-DFTB calculations. Results showed that hydrated structures are more compact with respect to a gas phase structures (Fig. 1b-d): long carbon chains (with carboxylic groups in the ends) interact with water molecules and became folded. Additionally, it seems the solvation of the molecule is not uniform. Indeed, it is possible that longer simulation of dynamics would have shown some different situations, but present results seem consistent with the fact that carbon chains involved poor solvation interaction and therefore the solvation is stronger for other side of the molecule.

• Ionized form of m-CDOM model $(C_{48}O_{19}N_1H_{72}^-)\cdot(H_2O)_{100}$. There are 3 carboxylic groups in the $C_{48}O_{19}N_1H_{73}\cdot(H_2O)_{100}$ system, Fig. 1a. These group participate in two types of possible interactions: (i) interactions between two nearest -COOH groups (Fig. 1e); and (ii) interactions of -COOH groups with water molecules (usually 3 or 4 water molecules) (Fig. 1f).

However, in all MD trajectories calculated for hydrated species, the proton migration process from -COOH groups and water molecules was not seen. This is probably due to the weak acidic nature of m-CDOM and 20 ps of calculation time per MD trajectory, which is probably not enough for ionization process occurs. To study the impact of the deprotonated form of m-CDOM to the total optical spectrum, several ionized structures $(C_{48}O_{19}N_1H_{72}^-)\cdot(H_2O)_{100}$ were simulated (Fig. S2, ESI†). To get geometries for these systems, one neutral structure of C₄₈O₁₉N₁H₇₃·(H₂O)₁₀₀ was selected from the MD trajectories, and the proton was removed from each carboxylic group, that allowed us to get three different ionized molecules $(C_{48}O_{19}N_1H_{72}^-)\cdot(H_2O)_{100}$ (Fig. S2a-c, ESI†). Then geometry optimization procedure was performed for all three (C₄₈O₁₉N₁H₇₂⁻) (H₂O)₁₀₀ structures. These equilibrium geometries were used for simulation of optical absorption spectrum of ionized species.

Author contributions

Natalia V. Karimova performed theoretical simulations; Michael Alves and Man Luo made experimental measurements. Vicki H. Grassian (experimental aspects) and R. Benny Gerber (theoretical aspects) participated in the analysis of results and conclusions and are corresponding authors. All authors contributed to either the writing and/or editing of the manuscript.

Data availability

Additional data related to this paper can be accessed from the UC San Diego Library Digital Collections (https://doi.org/10.6075/J0M90775) or may be requested from the authors.

Conflicts of interest

There are no conflicts to declare.

Acknowledgements

The authors would like to gratefully acknowledge supported by the National Science Foundation through the Center for Aerosol Impacts on Chemistry of the Environment funded under the Centers for Chemical Innovation Program Grant CHE1801971. Additionally, this work used the Extreme Science and Engineering Discovery Environment (XSEDE),⁷⁹ which is supported by grant number TG-CHE170064. The authors would also like to thank Professor Juan Navea for helpful discussions. Also, the authors gratefully acknowledge Dr. Samantha Doyle and Professor Michael Tauber for the use of their UV-VIS spectrometer and helping us concentrate the marine-derived chromophoric dissolved organic sample, as well as the whole SeaSCAPE 2019 team that made much of this work possible, specifically Kimberly Prather, Christopher Cappa, Timothy Bertram, Jonathan Sauer, and Kathryn Mayer for their leadership in this experiment.

References

PCCP

- 1 D. J. Hassett, M. S. Bisesi and R. Hartenstein, Bactericidal action of humic acids, Soil Biol. Biochem., 1987, 19, 111-113.
- 2 M. Klavins and O. Purmalis, Humic substances as surfactants, Environ. Chem. Lett., 2010, 8, 349-354.
- 3 J. A. Rice and P. MacCarthy, Statistical evaluation of the elemental composition of humic substances, Org. Geochem., 1991, 17, 635-648.
- 4 C. E. J. van Rensburg, The antiinflammatory properties of humic substances: a mini review, Phytother. Res., 2015, 29, 791-795.
- 5 M. Zark and T. Dittmar, Universal molecular structures in natural dissolved organic matter, Nat. Commun., 2018, 9, 3178.
- 6 J. D. Kinsey, G. Corradino, K. Ziervogel, A. Schnetzer and C. L. Osburn, Formation of chromophoric dissolved organic matter by bacterial degradation of phytoplankton-derived aggregates, Front. Mater. Sci., 2018, 4, 430.
- 7 M. R. Shields, T. S. Bianchi, C. L. Osburn, J. D. Kinsey, K. Ziervogel, A. Schnetzer and G. Corradino, Linking chromophoric organic matter transformation with biomarker indices in a marine phytoplankton growth and degradation experiment, Mar. Chem., 2019, 214, 103665.
- 8 P. K. Quinn, D. B. Collins, V. H. Grassian, K. A. Prather and T. S. Bates, Chemistry and related properties of freshly emitted sea spray aerosol, Chem. Rev., 2015, 115, 4383-4399.
- 9 D. J. Carlson, Dissolved organic materials in surface microlayers: Temporal and spatial variability and relation to sea state: Microlayer DOM, Limnol. Oceanogr., 1983, 28, 415-431.
- 10 M. van Pinxteren, S. Barthel, K. W. Fomba, K. Müller, W. von Tümpling and H. Herrmann, The influence of environmental drivers on the enrichment of organic carbon in the sea surface microlayer and in submicron aerosol particles measurements from the Atlantic Ocean, Elementa: Science of the Anthropocene, 2017, 5, 35.
- 11 A. Nebbioso and A. Piccolo, Molecular characterization of dissolved organic matter (DOM): a critical review, Anal. Bioanal. Chem., 2013, 405, 109-124.
- 12 M. Denis, L. Jeanneau, A.-C. Pierson-Wickman, G. Humbert, P. Petitjean, A. Jaffrézic and G. Gruau, A comparative study on the pore-size and filter type effect on the molecular composition of soil and stream dissolved organic matter, Org. Geochem., 2017, 110, 36-44.
- 13 D. J. Repeta, Biogeochemistry of Marine Dissolved Organic Matter, Elsevier, 2015, pp. 21-63.
- 14 D. Durce, N. Maes, C. Bruggeman and L. Van, Ravestyn, Alteration of the molecular-size-distribution of Boom Clay dissolved organic matter induced by Na⁺ and Ca²⁺, J. Contam. Hydrol., 2016, 185-186, 14-27.
- 15 B. A. G. de Melo, F. L. Motta and M. H. A. Santana, Humic acids: Structural properties and multiple functionalities for novel technological developments, Mater. Sci. Eng., C, 2016, **62**, 967-974.
- 16 H. Kipton, J. Powell and R. M. Town, Solubility and fractionation of humic acid; effect of pH and ionic medium, Anal. Chim. Acta, 1992, 267, 47-54.

- 17 A. Mostovaya, J. A. Hawkes, T. Dittmar and L. J. Tranvik, Molecular determinants of dissolved organic matter reactivity in lake water, Front. Earth Sci., 2017, 5, 106.
- 18 E. B. Kujawinski, R. Del Vecchio, N. V. Blough, G. C. Klein and A. G. Marshall, Probing molecular-level transformations of dissolved organic matter: insights on photochemical degradation and protozoan modification of DOM from electrospray ionization Fourier transform ion cyclotron resonance mass spectrometry, Mater. Chem., 2004, 92, 23-37.
- 19 E. B. Kujawinski, K. Longnecker, N. V. Blough, R. D. Vecchio, L. Finlay, J. B. Kitner and S. J. Giovannoni, Identification of possible source markers in marine dissolved organic matter using ultrahigh resolution mass spectrometry, Geochim. Cosmochim. Acta, 2009, 73, 4384-4399.
- 20 K. Mopper, A. Stubbins, J. D. Ritchie, H. M. Bialk and P. G. Hatcher, Advanced instrumental approaches for characterization of marine dissolved organic matter: extraction techniques, mass spectrometry, and nuclear magnetic resonance spectroscopy, Chem. Rev., 2007, 107, 419-442.
- 21 B. P. Koch, M. Witt, R. Engbrodt, T. Dittmar and G. Kattner, Molecular formulae of marine and terrigenous dissolved organic matter detected by electrospray ionization Fourier transform ion cyclotron resonance mass spectrometry, Geochim. Cosmochim. Acta, 2005, 69, 3299-3308.
- 22 N. Hertkorn, M. Harir, B. P. Koch, B. Michalke and P. Schmitt-Kopplin, High-field NMR spectroscopy and FTICR mass spectrometry: powerful discovery tools for the molecular level characterization of marine dissolved organic matter, Biogeosciences, 2013, 10, 1583-1624.
- 23 W. S. Wan Ngah, M. A. K. M. Hanafiah and S. S. Yong, Adsorption of humic acid from aqueous solutions on crosslinked chitosan-epichlorohydrin beads: Kinetics and isotherm studies, Colloids Surf., B, 2008, 65, 18-24.
- 24 D. Kwon, M. J. Sovers, V. H. Grassian, P. D. Kleiber and M. A. Young, Optical properties of humic material standards: solution phase and aerosol measurements, ACS Earth Space Chem., 2018, 2, 1102-1111.
- 25 F. Nasser and I. Lynch, Secreted protein eco-corona mediates uptake and impacts of polystyrene nanoparticles on Daphnia magna, J. Proteomics, 2016, 137, 45-51.
- 26 S. Jayalath, H. Wu, S. C. Larsen and V. H. Grassian, Surface adsorption of suwannee river humic acid on TiO2 nanoparticles: a study of pH and particle size, Langmuir, 2018, 34, 3136-3145.
- 27 P. Coble, Marine optical biogeochemistry: the chemistry of ocean color, Chem. Rev., 2007, 107, 402-418.
- 28 D. A. Hansell and C. A. Carlson, Biogeochemistry of marine dissolved organic matter, Academic Press, Amsterdam, Boston, 2002.
- 29 E. S. Boyle, N. Guerriero, A. Thiallet, R. D. Vecchio and N. V. Blough, Optical properties of humic substances and CDOM: relation to structure, Environ. Sci. Technol., 2009, 43, 2262-2268.
- 30 J. V. Trueblood, M. R. Alves, D. Power, M. V. Santander, R. E. Cochran, K. A. Prather and V. H. Grassian, Shedding light on photosensitized reactions within marine-relevant organic thin films, ACS Earth Space Chem., 2019, 3, 1614-1623.

Paper

31 K. McNeill and S. Canonica, Triplet state dissolved organic matter in aquatic photochemistry: reaction mechanisms, substrate scope, and photophysical properties, *Environ. Sci.: Processes Impacts*, 2016, **18**, 1381–1399.

- 32 C. Baduel, D. Voisin and J.-L. Jaffrezo, Seasonal variations of concentrations and optical properties of water soluble HULIS collected in urban environments, *Atmos. Chem. Phys.*, 2010, **10**, 4085–4095.
- 33 A. Hoffer, A. Gelencsér, P. Guyon, G. Kiss, O. Schmid, G. P. Frank, P. Artaxo and M. O. Andreae, Optical properties of humic-like substances (HULIS) in biomass-burning aerosols, *Atmos. Chem. Phys.*, 2006, 6, 3563–3570.
- 34 Y.-P. Chin, G. Aiken and E. O'Loughlin, Molecular weight, polydispersity, and spectroscopic properties of aquatic humic substances, *Environ. Sci. Technol.*, 1994, **28**, 1853–1858.
- 35 D. P. Veghte, S. China, J. Weis, L. Kovarik, M. K. Gilles and A. Laskin, Optical properties of airborne soil organic particles, *ACS Earth Space Chem.*, 2017, 1, 511–521.
- 36 K. Kumada, Absorption spectra of humic acids, *Soil Sci. Plant Nutr.*, 1955, 1, 29–30.
- 37 X. Lei, J. Pan and A. Devlin, Characteristics of absorption spectra of chromophoric dissolved organic matter in the pearl river estuary in spring, *Remote Sens.*, 2019, 11, 1533.
- 38 J. Ma, R. Del Vecchio, K. S. Golanoski, E. S. Boyle and N. V. Blough, Optical properties of humic substances and CDOM: effects of borohydride reduction, *Environ. Sci. Tech*nol., 2010, 44, 5395–5402.
- 39 E. S. Boyle, N. Guerriero, A. Thiallet, R. D. Vecchio and N. V. Blough, Optical properties of humic substances and CDOM: relation to structure, *Environ. Sci. Technol.*, 2009, 43, 2262–2268.
- 40 M. Peacock, C. D. Evans, N. Fenner, C. Freeman, R. Gough, T. G. Jones and I. Lebron, UV-visible absorbance spectroscopy as a proxy for peatland dissolved organic carbon (DOC) quantity and quality: considerations on wavelength and absorbance degradation, *Environ. Sci.: Processes Impacts*, 2014, 16, 1445.
- 41 H. E. Reader, C. A. Stedmon, N. J. Nielsen and E. S. Kritzberg, Mass and UV-visible spectral fingerprints of dissolved organic matter: sources and reactivity, *Front. Mater. Sci.*, 2015, 2, 88, DOI: 10.3389/fmars.2015.00088.
- 42 C. M. Sharpless and N. V. Blough, The importance of charge-transfer interactions in determining chromophoric dissolved organic matter (CDOM) optical and photochemical properties, *Environ. Sci.: Processes Impacts*, 2014, **16**, 654–671.
- 43 C. George, M. Ammann, B. D'Anna, D. J. Donaldson and S. A. Nizkorodov, Heterogeneous photochemistry in the atmosphere, *Chem. Rev.*, 2015, **115**, 4218–4258.
- 44 K. Mopper, A. Stubbins, J. D. Ritchie, H. M. Bialk and P. G. Hatcher, Advanced Instrumental Approaches for Characterization of Marine Dissolved Organic Matter: Extraction Techniques, Mass Spectrometry, and Nuclear Magnetic Resonance Spectroscopy, *Chem. Rev.*, 2007, 107, 419–442.
- 45 J. A. Tossell, Quinone-hydroquinone complexes as model components of humic acids: theoretical studies of their

- structure, stability and Visible-UV spectra, *Geochim. Cosmo-chim. Acta*, 2009, **73**, 2023–2033.
- 46 E. A. Vialykh, G. McKay and F. L. Rosario-Ortiz, Computational assessment of the three-dimensional configuration of dissolved organic matter chromophores and influence on absorption spectra, *Environ. Sci. Technol.*, 2020, 54, 15904–15913.
- 47 R. Del Vecchio and N. V. Blough, On the origin of the optical properties of humic substances, *Environ. Sci. Technol.*, 2004, 38, 3885–3891.
- 48 C. N. Albers, G. T. Banta, O. S. Jacobsen and P. E. Hansen, Characterization and structural modelling of humic substances in field soil displaying significant differences from previously proposed structures, *Eur. J. Soil Sci.*, 2008, **59**, 693–705.
- 49 Y. S. S. Al-Faiyz, CPMAS ¹³C NMR characterization of humic acids from composted agricultural Saudi waste, *Arabian J. Chem.*, 2017, **10**, S839–S853.
- 50 J. Kosaka, C. Honda and A. Izeki, Fractionation of humic acid by organic solvents, *Soil Sci. Plant Nutr.*, 1961, 7, 48–53.
- 51 R. J. Kieber, L. H. Hydro and P. J. Seaton, Photooxidation of triglycerides and fatty acids in seawater: Implication toward the formation of marine humic substances, *Limnol. Oceanogr.*, 1997, **42**, 1454–1462.
- 52 M. A. Poshelyuzhnaya, V. A. Litvin, R. L. Galagan and B. F. Minaev, Quantum-chemical simulation of the synthesis of structural fragments of humic substances analogs, *Russ. J. Gen. Chem.*, 2014, **84**, 848–852.
- 53 S. A. Jansen, M. Malaty, S. Nwabara, E. Johnson, E. Ghabbour, G. Davies and J. M. Varnum, Structural modeling in humic acids, *Mater. Sci. Eng.*, C, 1996, 4, 175–179.
- 54 N. V. Karimova, M. Luo, V. H. Grassian and R. B. Gerber, Absorption spectra of benzoic acid in water at different pH and in the presence of salts: insights from the integration of experimental data and theoretical cluster models, *Phys. Chem. Chem. Phys.*, 2020, 22, 5046–5056.
- 55 K. Z. Aregahegn, M. J. Ezell and B. J. Finlayson-Pitts, Photochemistry of solid films of the neonicotinoid nitenpyram, *Environ. Sci. Technol.*, 2018, 52, 2760–2767.
- 56 K. Z. Aregahegn, D. Shemesh, R. B. Gerber and B. J. Finlayson-Pitts, Photochemistry of thin solid films of the neonicotinoid imidacloprid on surfaces, *Environ. Sci. Technol.*, 2017, 51, 2660–2668.
- 57 D. Porezag, Th Frauenheim, Th Köhler, G. Seifert and R. Kaschner, Construction of tight-binding-like potentials on the basis of density-functional theory: Application to carbon, *Phys. Rev. B: Condens. Matter Mater. Phys.*, 1995, **51**, 12947–12957.
- 58 T. A. Niehaus, S. Suhai, F. Della Sala, P. Lugli, M. Elstner, G. Seifert and T. Frauenheim, Tight-binding approach to time-dependent density-functional response theory, *Phys. Rev. B: Condens. Matter Mater. Phys.*, 2001, 63, 085108.
- 59 Y. Gao, M. Yan and G. V. Korshin, Effects of Ionic Strength on the Chromophores of Dissolved Organic Matter, *Environ. Sci. Technol.*, 2015, 49, 5905–5912.
- 60 P. Jungwirth and B. Winter, Ions at aqueous interfaces: from water surface to hydrated proteins, *Annu. Rev. Phys. Chem.*, 2008, **59**, 343–366.

- 61 X. Wang, C. M. Sultana, J. Trueblood, T. C. J. Hill, F. Malfatti, C. Lee, O. Laskina, K. A. Moore, C. M. Beall, C. S. McCluskey, G. C. Cornwell, Y. Zhou, J. L. Cox, M. A. Pendergraft, M. V. Santander, T. H. Bertram, C. D. Cappa, F. Azam, P. J. DeMott, V. H. Grassian and K. A. Prather, Microbial control of sea spray aerosol composition: a tale of two blooms, ACS Cent. Sci., 2015, 1, 124-131.
- 62 T. Dittmar, B. Koch, N. Hertkorn and G. Kattner, A simple and efficient method for the solid-phase extraction of dissolved organic matter (SPE-DOM) from seawater: SPE-DOM from seawater, Limnol. Oceanogr.: Methods, 2008, 6, 230-235.
- 63 H. Zhou, E. Tajkhorshid, T. Frauenheim, S. Suhai and M. Elstner, Performance of the AM1, PM3, and SCC-DFTB methods in the study of conjugated Schiff base molecules, Chem. Phys., 2002, 277, 91-103.
- 64 M. Berdakin, M. Taccone, K. J. Julian, G. Pino and C. G. Sánchez, Disentangling the photophysics of DNAstabilized silver nanocluster emitters, J. Phys. Chem. C, 2016, 120, 24409-24416.
- 65 J. Frenzel, J.-O. Joswig and G. Seifert, Optical excitations in cadmium sulfide nanoparticles, J. Phys. Chem. C, 2007, 111, 10761-10770.
- 66 F. Alkan and C. M. Aikens, TD-DFT and TD-DFTB investigation of the optical properties and electronic structure of silver nanorods and nanorod dimers, J. Phys. Chem. C, 2018, 122, 23639-23650.
- 67 B. Hourahine, B. Aradi, V. Blum, F. Bonafé, A. Buccheri, C. Camacho, C. Cevallos, M. Y. Deshaye, T. Dumitrică, A. Dominguez, S. Ehlert, M. Elstner, T. van der Heide, J. Hermann, S. Irle, J. J. Kranz, C. Köhler, T. Kowalczyk, T. Kubař, I. S. Lee, V. Lutsker, R. J. Maurer, S. K. Min, I. Mitchell, C. Negre, T. A. Niehaus, A. M. N. Niklasson, A. J. Page, A. Pecchia, G. Penazzi, M. P. Persson, J. Řezáč, C. G. Sánchez, M. Sternberg, M. Stöhr, F. Stuckenberg, A. Tkatchenko, V. W.-Z. Yu and T. Frauenheim, DFTB⁺, a software package for efficient approximate density functional theory based atomistic simulations, J. Chem. Phys., 2020, 152, 124101.
- M. Gaus, Q. Cui and M. Elstner, DFTB3: Extension of the Self-Consistent-Charge Density-Functional Tight-Binding Method (SCC-DFTB), J. Chem. Theory Comput., 2011, 7, 931-948.

- 69 J. Řezáč, Empirical self-consistent correction for the description of hydrogen bonds in DFTB3, J. Chem. Theory Comput., 2017, 13, 4804-4817.
- 70 M. Gaus, X. Lu, M. Elstner and O. Cui, Parameterization of DFTB3/3OB for sulfur and phosphorus for chemical and biological applications, J. Chem. Theory Comput., 2014, 10, 1518-1537.
- 71 M. Kubillus, T. Kubař, M. Gaus, J. Řezáč and M. Elstner, Parameterization of the DFTB3 method for Br, Ca, Cl, F, I, K, and Na in organic and biological systems, J. Chem. Theory Comput., 2015, 11, 332-342.
- 72 M. Gaus, A. Goez and M. Elstner, Parametrization and benchmark of DFTB3 for organic molecules, J. Chem. Theory Comput., 2013, 9, 338-354.
- 73 X. Lu, M. Gaus, M. Elstner and O. Cui, Parametrization of DFTB3/3OB for Magnesium and Zinc for Chemical and Biological Applications, J. Phys. Chem. B, 2015, 119, 1062-1082.
- 74 J. Řezáč and P. Hobza, Advanced corrections of hydrogen bonding and dispersion for semiempirical quantum mechanical methods, J. Chem. Theory Comput., 2012, 8, 141-151.
- 75 D. E. Romonosky, L. Q. Nguyen, D. Shemesh, T. B. Nguyen, S. A. Epstein, D. B. C. Martin, C. D. Vanderwal, R. B. Gerber and S. A. Nizkorodov, Absorption spectra and aqueous photochemistry of β-hydroxyalkyl nitrates of atmospheric interest, Mol. Phys., 2015, 113, 2179-2190.
- 76 D. Shemesh, M. Luo, V. H. Grassian and R. B. Gerber, Absorption spectra of pyruvic acid in water: insights from calculations for small hydrates and comparison to experiment, Phys. Chem. Chem. Phys., 2020, 22, 12658-12670.
- 77 M. Luo, D. Shemesh, M. N. Sullivan, M. R. Alves, M. Song, R. B. Gerber and V. H. Grassian, Impact of pH and NaCl and CaCl₂ salts on the speciation and photochemistry of pyruvic acid in the aqueous phase, J. Phys. Chem. A, 2020, 124, 5071–5080.
- 78 L. Martínez, R. Andrade, E. G. Birgin and J. M. Martínez, PACK-MOL: a package for building initial configurations for molecular dynamics simulations, J. Comput. Chem., 2009, 30, 2157-2164.
- 79 J. Towns, T. Cockerill, M. Dahan, I. Foster, K. Gaither, A. Grimshaw, V. Hazlewood, S. Lathrop, D. Lifka, G. D. Peterson, R. Roskies, J. R. Scott and N. Wilkens-Diehr, XSEDE: Accelerating Scientific Discovery, Comput. Sci. Eng., 2014, 16, 62-74.